RSC Advances

ROYAL SOCIETY OF CHEMISTRY

www.rsc.org/advances

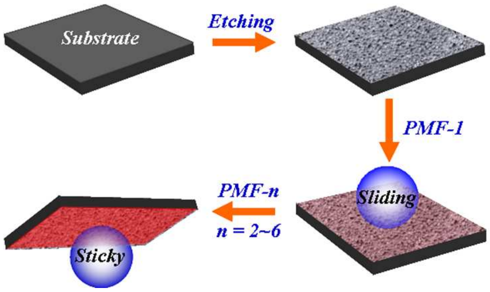

The superoleophobic surfaces with controllable liquid adhesion from sliding state to sticky state were obtained by the deposition of polyelectrolyte multilayer films on the micro/nanostructured substrates.

Fabrication of superoleophobic surfaces with controllable liquid adhesion from polyelectrolyte multilayer film

Jin Yang[a]*, Haojie Song[a], Beibei Chen[a], Hua Tang[a], Changsheng Li[a]

[a] *Institute for Advanced Materials, School of Materials Science and Engineering, Jiangsu University, Zhenjiang, 212013, P.R. China*

Abstract

Superoleophobic surfaces with controllable liquid adhesion were developed on the micro/nanostructured aluminum substrates through the deposition of polyelectrolyte multilayer films ion-paired with perfluorooctanoate anions. Various liquids, such as water, glycerol, rapeseed oil, and hexadecane, can be tuned from rolling state to pinned state on the superoleophobic surfaces with increasing the number of polyelectrolyte bilayers. The effects of chemical heterogeneity and topographic roughness of polyelectrolyte deposited substrates on liquid adhesion properties were systematically studied. The combined effect of surface chemical defects coupled with the disappearance of nanoflakes and the interconnection of protrusions with the polyelectrolyte deposition led to the surfaces change from sliding superoleophobicity to sticky superoleophobicity. Our results gave a useful attempt in understanding the fabrication principle of preparing superoleophobic surfaces with controllable liquid adhesion. Moreover, the function of controllable liquid adhesion from polyelectrolyte multilayer film could potentially be used in important applications, such as in the selection and transportation of microdroplets.

Keywords: superoleophobicity, liquid adhesion, polyelectrolyte

---

*E-mail: yangjin@mail.ujs.edu.cn

1. Introduction

Superoleophobic surfaces, that exhibit non-wetting behaviors for both water and oil, have attracted significant interest because of their potential applications in many fields, including fluid transfer, antifouling and anticrawling materials, water-oil repellent fabrics, and microfluidic applications.[1-4] In these applications, controlling liquid adhesion on the target surface is of particular importance. Low adhesion to liquid droplets on the superoleophobic surfaces is favor to the surface antifouling. High liquid adhesion could expand their applications in the fields such as no-loss microdroplet transfer and trance-liquid reactors. Many studies about superoleophobicity usually focus on improving the contact angle values of low surface tension liquids, while few reports involved liquid adhesive properties.[5-8] This is because low surface tension liquids tend to easily wet the solid surfaces, making the control of liquid adhesion very difficult. Until recently, various research groups have tried to develop superoleophobic surfaces with low adhesion by using stainless steel meshes as substrates or by introducing some specially designed patterns, such as overhang structures and re-entrant surface curvatures.[9-14] However, studies of controlling liquid adhesion on superoleophobic surfaces are still rare.

The adhesion between the surfaces and liquid droplets are dependent on their surface morphologies and chemical compositions. Many studies on tunable water adhesion of superhydrophobic surfaces in response to changes of surface microstructure and composition have been reported.[15-18] Moreover, there are three wetting states to describe the liquid adhesion on rough surface: Wenzel’s state, Cassie-Baxter’s state, and the transitional state.[19] In Wenzel’s state, the liquid droplets often pin on the surface in a wet contact mode and cannot roll off the surface.[20] Conversely, in Cassie-Baxter's state, the liquid droplets adopt a non-wet contact mode on solid surface and can roll off easily owing to their low adhesive force.[21] Additionally, the wetting behaviors of the transitional state is between Wenzel's and Cassie-Baxter's state, and liquid droplet mobility in this state is determined by solid liquid interface contact area and three phase contact line.[22] Therefore, through dynamically tuning the surface structure and composition to locate the wetting states, liquid adhesion on superoleophobic surfaces could be precise controlled.

Recently, Jiang et al. fabricated superoleophobic surfaces with controllable surface morphologies, and investigated the topographic effect on oil adhesion ability.[23] Zhou et al. realized the reversible adhesion of glycerol droplets on superoleophobic TiO_2 surface through the alternate treatment by UV and annealing and discussed the chemical effect on the adhesion of glycerol.[24] Meanwhile, we also realized the tunable adhesion with various liquids on the superoleophobic surface by masked plasma treatment and surface fluorination.[25] Despite this progress in fabrication of superoleophobic surfaces, a systematic study of the effects of chemical heterogeneity and topographic roughness on liquid adhesion is still highly desirable.

Due to the changeful of the self-assembly way and chemical structure, polyelectrolyte film has been used to fabricate superhydrophobic and superoleophobic surfaces and tune their surface wettability.[26-30] In the present study, we systematically investigate the relationship between liquid adhesion and chemical defects and surface topographic features by the fabrication and characterization of polyelectrolyte multilayer film (PMF) on the micro/nanostructured substrate. The gradual changes of surface structure and chemical composition induced by increasing polyelectrolyte bilayers led to the surfaces tune from sliding superoleophobicity to sticky superoleophobicity for various liquids, such as water, glycerol, rapeseed oil, and hexadecane. The details of the controllable liquid adhesion from PMF was described herein.

2. Experimental section

2.1 Materials

Poly(sodium 4-styrene sulfonate) (PSS, Mw = 70 000), poly(diallydimethylammonium chloride) (PDDA, Mw = 200 000-350 000), and perfluorooctanoic acid ($CF_3(CF_2)_6COOH$) were all purchased from Sigma-Aldrich. Pure aluminum (AR, 99.5%), sodium chloride (NaCl) and sodium hydroxide (NaOH) were purchased from Sinopharm Chemical Reagent Co., Ltd. and used as received. Sodium perfluorooctanoate (PFO) (0.10 M) was prepared by the reaction of perfluorooctanoic acid with NaOH in water.

2.2 Preparation of micro/nanostructured substrate

An aluminum plate ($20 \times 20 \times 0.25$ mm^3) was cleaned ultrasonically with acetone and ethanol to get rid of grease. The cleaned aluminum plate was etched in a 2.5 M HCl solution for 10 min at room temperature. After being rinsed with deionized water, the sample was immersed in boiling deionized water for 30 min and subsequently dried with nitrogen.

2.3 Preparation of PMFs on the textured substrate

The polyelectrolyte deposition was performed following a literature procedure.[31] The textured substrate was immersed in PDDA (1.0 mg/mL, with 1.0 M NaCl present) aqueous solutions for 10 min to obtain a positively charged surface. Then, the PDDA-modified substrate was immersed in PSS (1.0 mg/mL, with 1.0 M NaCl present) aqueous solutions for

10 min, followed by rinsing with water. This cycle of PDDA treatment followed by PSS treatment was repeated to obtain the PMF-n with PDDA as the cap layer on the surface, where n represents the number of deposition cycles. Subsequently, the polyelectrolyte deposited substrates were immersed in an aqueous PFO solution (0.1M) for 1 min, followed by rinsing with deionized water and drying with nitrogen. In this work, the contact angles and sliding angles were always measured after the PMF-n coordinated with PFO anions.

2.4 Characterization

Scanning electron microscopy measurements were carried out using a JSM-6701F field-emission scanning electron microscopy (FESEM, JEOL, Japan). X-ray photoelectron spectroscopy (XPS) analysis of the sample was performed on a PHI-5702 electron spectrometer using an Al Kα line excitation source with the reference of C 1s at 285.0 eV. Contact angle and sliding angle measurements were performed using a Krüss DSA 100 (Krüss Company, Ltd., Germany) apparatus at ambient temperature. The volumes of various liquids in all measurements were approximately 5 μL. The images of liquid droplets on the aluminum surface were captured with a traditional digital camera (Canon).

3. Results and discussion

The surface micro/nanostructure is an important factor to obtain superoleophobicity. By the combination of the etching and boiling water treatment, hierarchical rough surface structures composed of protrusions, pores, and a number of distorted nanoflakes were obtained on the aluminum substrate (Figure 1a-c). The substrate surface is superhydrophilic and superoleophilic without any chemical modification. After the deposition of PMF-1 coordinated with PFO anions, the surface morphology of micro/nanostructured substrate shows no apparent change as shown in Figure 1d-e. However, the surface wettability changes to superhydrophobicity and superoleophobicity by displaying contact angles greater than 150° with liquids possessing significantly lower surface tension, such as hexadecane.

The superoleophobicity of the polyelectrolyte deposited substrate is highlighted in Figure 2a, which shows that droplets of different liquids (water, glycerol, rapeseed oil, and hexadecane) exhibit typical spherical shapes on the surface. The bright and reflective surface visible underneath the liquid droplets is a signature of trapped air and the composite solid-liquid-air interfaces established between the liquid droplets and the superoleophobic surface.[32] The contact angle values reach to 160 ± 0.5°, 159 ± 0.6°, 156 ± 0.9°, and 156 ± 0.9° for these liquids respectively, as shown in Figure 2b. Furthermore, liquid droplets can roll off the surface easily by tilting to certain angle (< 10°), exhibiting very low liquid adhesion on this superoleophobic surface. Figure 2c shows the start rolling images of these liquid droplets in the sliding angle measurement. This low liquid adhesion can be attributed to the existence of the trapped air between the solid surface and the liquids, and the liquid droplets are in the Cassie-Baxter state.

The change of chemical composition is the main factor to induce the highly enhanced oleophobicity and low liquid adhesion on the substrate after the deposition of PMF-1 coordinated with PFO anions. XPS was performed to investigate the surface chemistry of the samples, which indicated the elemental existence of C and F on the prepared surface (Figure 3a). These signals in the survey spectrum can be attributed to the adsorbed polyelectrolytes and PFO anions. The high resolution C1s core level spectrum (Figure 3b), resolved into three components, namely, $-CF_3$, $-CF_2$, and $-CH_2$, can also be regarded as another evidence. The fluoride content for the polyelectrolyte deposited substrate was mostly as high as 56%, indicating that this surface was mainly covered by fluorocarbons, which was the basis for the sliding superoleophobicity of the surfaces.

To control liquid adhesion of the superoleophobic surface, more cycles of polyelectrolyte deposition were performed onto the micro/nanostructured substrate. As shown in Figure 4, we measured the contact angles and sliding angles with hexadecane, rapeseed oil, glycerol, and water on the substrates deposited PMF-n (n=1~6). It can be seen that, with increasing the number of polyelectrolyte bilayers, all of the contact angles gradually decrease and all of the sliding angles increase until liquid droplets cannot roll off the surface. Importantly, at a given number of polyelectrolyte bilayers, the surface can display contact angle larger than 150° and high adhesion to a liquid. For example, on the PMF-2 surface, the contact angle of hexadecane decreased to 152 ± 0.8°, and a hexadecane droplet could be pinned under this surface even when inverting the surface (Figure 4a inset), exhibiting high liquid adhesion on the superoleophobic surface. However, other liquid droplets on this surface still remained their sliding behaviors. Similarly, on the PMF-3 and PMF-5 surfaces, we can get sticky superoleophobicity for rapeseed oil and glycerol, respectively (Figure 4b and c insets). For the PMF-6, the superoleophobic surface showed high adhesion behaviors to both glycerol and water (Figure 4c and d insets). The pinned phenomenon for glycerol and water can be observed on the same surface. In a word, through increasing the number of polyelectrolyte bilayers, tunable adhesion with various liquids from rolling state to pinned state can be obtained on the superoleophobic surface.

To understand the controllable liquid adhesion in superoleophobic state from PMF, the chemical heterogeneity of the surface after polyelectrolyte deposition is the first factor to discuss. As demonstrated previously,[33,34] lager numbers of surface defects, i.e. chemically heterogeneous domains, are always concomitant with the hydrophobized PMFs. The surface defects probably are formed via desorption of individual polyelectrolyte chains from the surface. Specifically, chemically heterogeneous domains on PMFs show a strong affinity to liquids surrounding them, which pin the three phase contact line of liquid droplet and result in extremely high liquid adhesion. However, the area fraction of defects decreases with the increase of the deposition cycles.[35] Through XPS analysis performed on the PMF-n carrying PFO anions (Figure 5), the fluoride content gradually increases from 56% for PMF-1 to 65% for PMF-6, indicating that some surface defects have been covered by PDDA/PFO units with increasing polyelectrolyte bilayers. Moreover, as the disappearance of surface defects, various liquid droplets on the superoleophobic surface contrary tuned from rolling state to pinned state. Therefore, the chemical heterogeneity may not be the main influencing factor on the high liquid adhesion behaviors of superoleophobic surfaces. Other influencing factor, i.e. topographic roughness, should play a very important role on the enhancement of liquid adhesion.

The surface morphology of micro/nanostructured substrate deposited PMF-n was viewed with FESEM. After PMF-2 deposition, it can been seen that protrusions in micrometer scale remain original structures, but the nanoflakes began to thicken due to the polyelectrolyte absorption (Figure 6a,b). Through the changes of nanoflakes, the thickness of PMF for each deposition cycle was estimated to be about 40 nm. When the polyelectrolyte was continually deposited onto the substrate to obtain PMF-3, the nanoflakes have been almost buried by polyelectrolyte, leading to only the edge of the nanoflakes appears on the original region (Figure 6c,d). For PMF-4, PMF-5, and PMF-6, the microscale protrusions began to interconnect resulting in the pores were filled gradually, meanwhile, the nanoflakes have been disappeared completely (Figure 6e-j). The disappearance of nanoflakes and the interconnection of protrusions after PMF deposition on the substrate can help to convert the composite solid-liquid-air interface from the Cassie-Baxter state to the transitional state, which causes the increase of solid-liquid interface contact area and the enhancement of liquid adhesion.

The function of controllable liquid adhesion from PMF could potentially be used in important applications, such as in the selection and transportation of microdroplets. For example, we placed four kinds of liquid droplets (water, glycerol, rapeseed oil, and hexadecane) on the PMF-1 surface. When the surface deposited different cycles of polyelectrolyte bilayers contacted with these liquid droplets from the above, a liquid droplet can adhere to the surface to be carried off and transferred. For the PMF-2 surface, a hexadecane droplet was successfully brought up, leaving other liquid droplets remain their original states (Figure 7a). As we used the PMF-3, PMF-5, and PMF-6 surfaces to contact these liquid droplets orderly, rapeseed oil (Figure 7b), glycerol (Figure 7c), and water (Figure 7d) could be selected effectively and transferred to other place without any loss, respectively.

4.Conclusions

In this paper, we have studied the effects of PMFs deposited on micro/nanostructured substrate on the liquid adhesion properties within superoleophobic state. After the deposition of PMF-1 coordinated with PFO anions, the surface micro/nanostructures obtained by the etching and boiling water treatment of the aluminum substrate, along with the high fluoride content of the surface, resulted in the sliding superoleophobicity for various liquids possessing significantly lower surface tension. With increasing the polyelectrolyte bilayers from 1 to 6, the combined effect of surface defects coupled with the disappearance of nanoflakes and the interconnection of protrusions led to the surfaces that displayed sticky superoleophobicity for various liquids, such as water, glycerol, rapeseed oil, and hexadecane. The superoleophobic surfaces with controllable liquid adhesion from sliding state to sticky state were obtained by the deposition of PMFs on the micro/nanostructured substrate. This result is particularly interesting given that the superoleophobic surfaces use to transport and select different liquid droplets as the "mechanical hand" and exhibit refined control of liquid droplet mobility for biological and microfluidic applications.

Acknowledgments

The authors are grateful for the financial support from China Postdoctoral Science Foundation (Grant No. 2013M530235), Jiangsu Key Lab of material tribology Foundation (Grant No. kjsmcx2012003), and the Senior Intellectuals Fund of Jiangsu University (Grant No. 12JDG092).

References

[1] A. K. Kota, W. Choi and A. Tuteja, *MRS Bull.*, 2013, 38, 383−390.

[2] S. Pan, A. K. Kota, J. M. Mabry and A. Tuteja, *J. Am. Chem. Soc.*, 2013, 135, 578−581.

[3] H. Wang, H. Zhou, A. Gestos, J. Fang and T. Lin, *ACS Appl. Mater. Interfaces*, 2013, 5, 10221−10226.

[4] K. Liu, Y. Tian and L. Jiang, *Prog. Mater. Sci.*, 2013, 58, 503–564.

[5] S. E. Lee, H. J. Kim, S. H. Lee and D. G. Choi, *Langmuir*, 2013, 29, 8070−8075.

[6] R. T. R. Kumar, K. B. Mogensen and P. Bøggild, *J. Phys. Chem. C*, 2010, 114, 2936–2940.

[7] L. Li, V. Breedveld and D. W. Hess, *ACS Appl. Mater. Interfaces*, 2013, 5, 5381−5386.

[8] Y. Liu, Y. Xiu, D. W. Hess and C. P. Wong, *Langmuir*, 2010, 26, 8908–8913.

[9] W. Wu, X. Wang, D. Wang, M. Chen, F. Zhou, W. Liu and Q. Xue, *Chem. Commun.*, 2009, 1043–1045.

[10] A. Tuteja, W. Choi, M. Ma, J. M. Mabry, S. A. Mazzella, G. C. Rutledge, G. H. McKinley and R. E. Cohen, *Science*, 2007, 318, 1618−1622.

[11] A. K. Kota, Y. Li, J. M.Mabry and A. Tuteja, *Adv. Mater.*, 2012, 24, 5837−5842.

[12] J. Zhang and S. Seeger, *Angew. Chem. Int. Ed.*, 2011, 50, 6652−6657.

[13] X. Deng, L. Mammen, H. J. Butt and D. Vollmer, *Science*, 2011, 335, 67−70.

[14] J. Ou, W. Hu, S. Liu, M. Xue, F. Wang and W. Li, *ACS Appl. Mater. Interfaces*, 2013, 5, 10035−10041.

[15] X. Liu, Y. Liang, F. Zhou and W. Liu, *Soft Matter*, 2012, 8, 2070−2086.

[16] X. Liu, Q. Ye, X. Song, Y. Zhu, X. Cao, Y. Liang and F. Zhou, *Soft Matte*r, 2011,7, 515–523.

[17] X. Liu, M. Cai, Y. Liang, F. Zhou and W. Liu, *Soft Matter*, 2011, 7, 3331–3336.

[18] Y. Wu, Y. Xue, X. Pei, M. Cai, H. Duan, W. T. S. Huck, F. Zhou and Q. Xue, *J. Phys. Chem. C*, 2014, 118, 2564−2569.

[19] S, Wang and L. Jiang, *Adv. Mater.*, 2007, 19, 3423–3424.

[20] R. N. Wenzel. *Ind. Eng. Chem.*, 1936, 28, 988–994.

[21] A. B. D. Cassie, and S. Baxter, *Trans. Faraday Soc.*, 1944, 40, 546–551.

[22] M. Nosonovsky and B. Bhushan, *Langmuir*, 2008, 24, 1525–1533.

[23] X. Yao, J. Gao, Y. Song and L. Jiang, *Adv. Mater.*, 2011, 21, 4270–4276.

[24] D. Wang, X. Wang, X. Liu and F. Zhou, *J. Phys. Chem. C*, 2010, 114, 9938–9944.

[25] J, Yang, H. J. Song, H. Tang, H. Y. Ji and C. S. Li, *Appl. Surf. Sci.*, 2013, 280, 940–944.

[26] H. S. Lim, S. G. Lee, D. H. Lee, D. Y. Lee, S. Lee and K. Cho, *Adv. Mater.*, 2008, 20, 4438–4441.

[27] C. H. Lee, S. K. Kang, J. A. Lim, Y. J. Kwark, H. S. Lim, J. Kim and J. H. Cho, *J. Mater. Chem.*, 2012, 22, 14656–14660.

[28] C. Jiang, Q. Wang and T. Wang, *New J. Chem.*, 2012,36, 1641–1645.

[29] L. Wang, B. Peng and Z. Su, *Langmuir*, 2010, 26, 12203–12208.

[30] J. Yang, Z. Z. Zhang X. H. Men, X. H. Xu, X. T. Zhu, X. Y. Zhou and Q. J. Xue, *J. Colloid Interface Sci.*, 2012, 366, 191–195.

[31] L. Wang, Y. Lin and Z. Su, *Soft Matter*, 2009, 5, 2072–2078.

[32] W. Choi, A. Tuteja, S. Chhatre, J. M. Mabry, R. E. Cohen and G. H. McKinley, *Adv. Mater.*, 2009, 21, 2190–2195.

[33] L. M. Wang, L. Wang and Z. H. Su, *Soft Matter*, 2011, 7, 4851–4855.

[34] R. M. Jisr, H. H. Rmaile and J. B.Schlenoff, *Angew. Chem. Int. Ed.*, 2005, 44, 782–785.

[35] L. M. Wang, J. J. Wei, Z. H. Su, *Langmuir*, 2011, 27, 15299–15304.

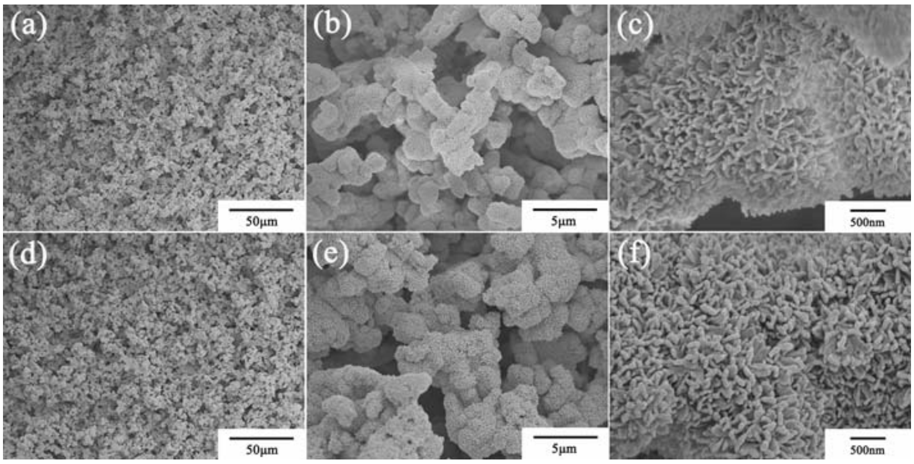

Figure 1. FESEM images of the micro/nanostructured aluminum substrate (a-c) before and (d-f) after PMF-1 deposition.

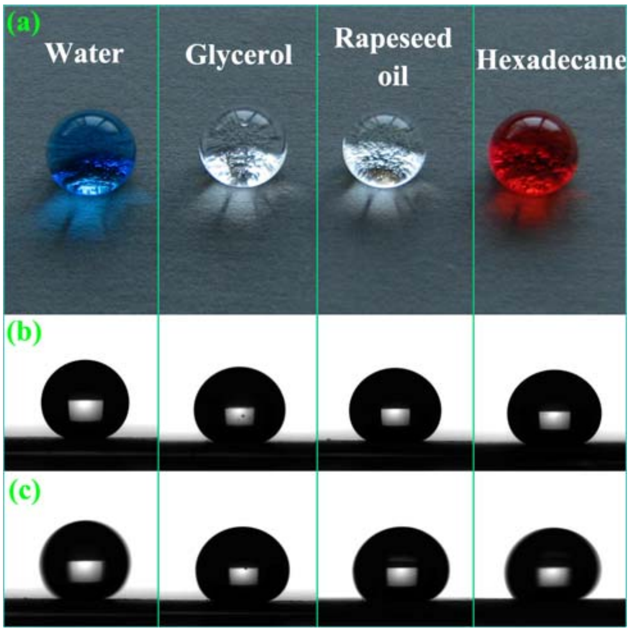

Figure 2. (a) Photographs of water, glycerol, rapeseed oil, and hexadecane droplets on the PMF-1deposited substrate. (b,c) Images of the above liquid droplets in the measurements of (b) contact angle and (c) sliding angle.

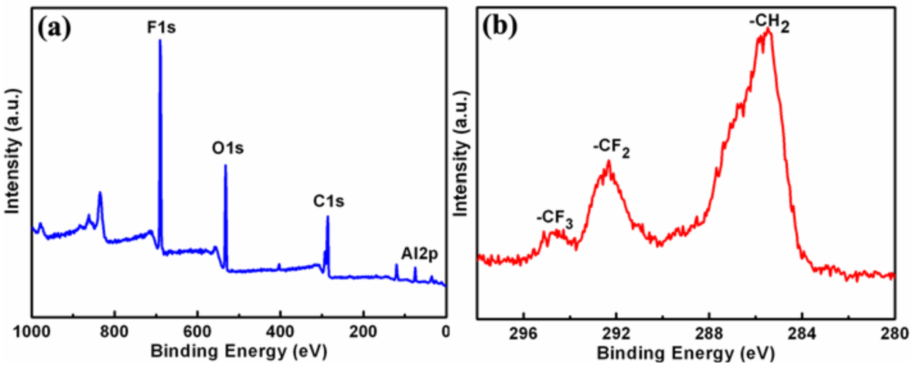

Figure 3. (a) XPS survey spectrum and (b) C 1s peaks of the PMF-1 deposited substrate.

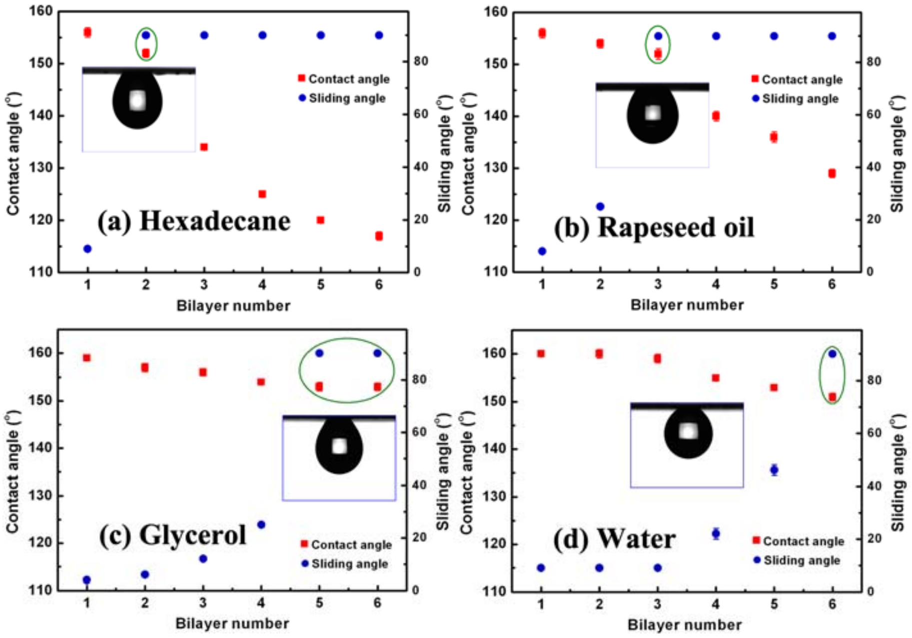

Figure 4. Contact angles and sliding angles for (a) hexadecane, (b) rapeseed oil, (c) glycerol, and (d) water on the PMF-n deposited substrates as a function of the number of polyelectrolyte bilayers (n). The insets show that liquid droplets pin under the surfaces.

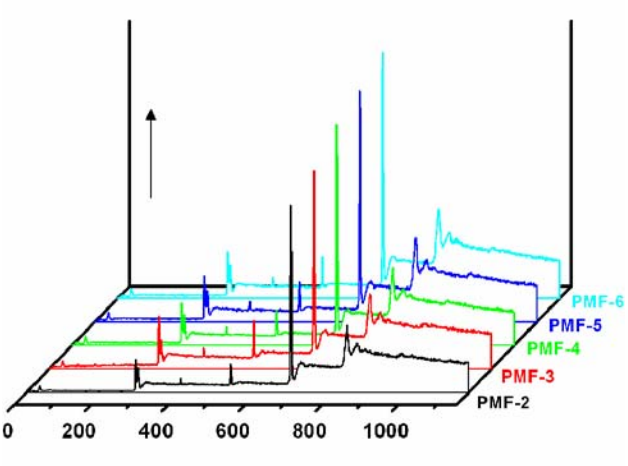

Figure 5. XPS survey spectra of the PMF-2, PMF-3, PMF-4, PMF-5, and PMF-6 deposited substrates.

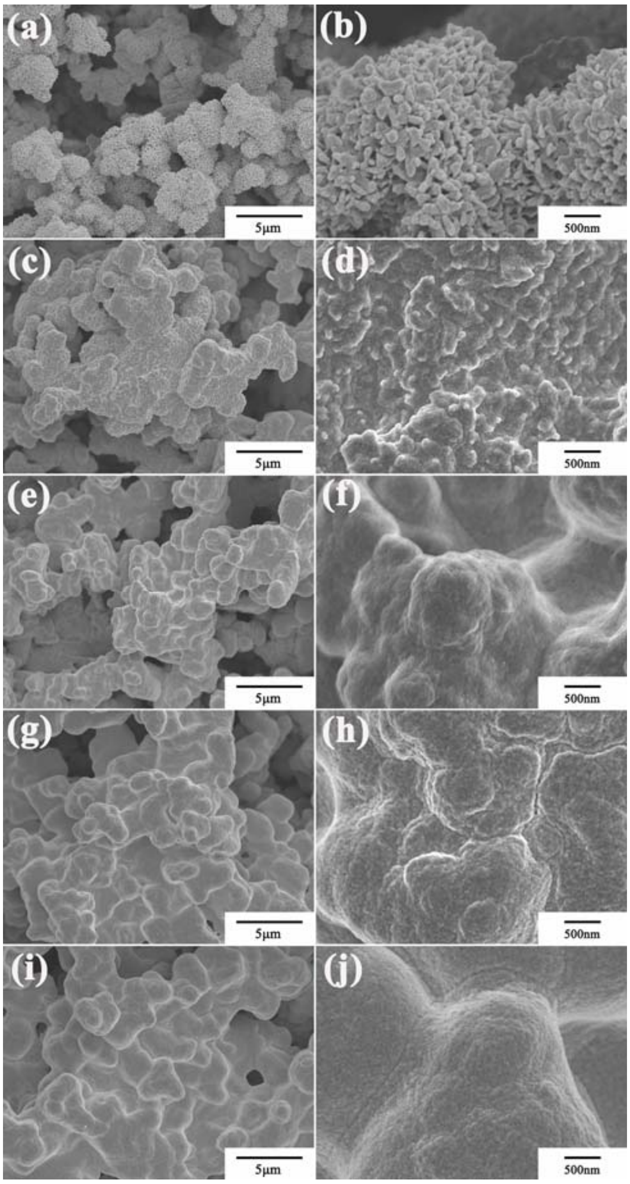

Figure 6. FESEM images of the PMF-n deposited substrates: (a,b) PMF-2, (c,d) PMF-3, (e,f) PMF-4, (g,h) PMF-5, and (i,j) PMF-6.

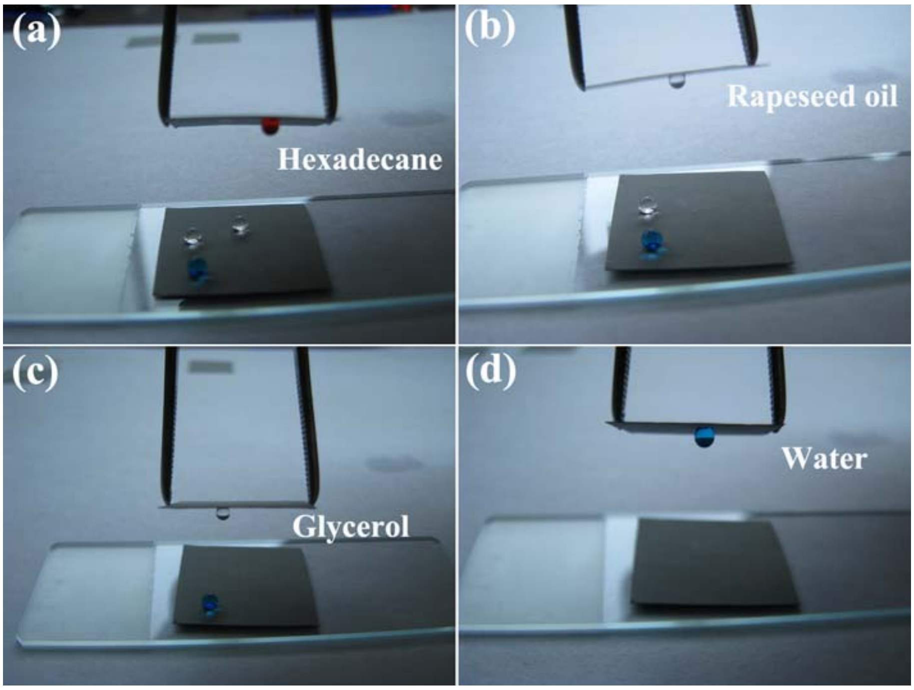

Figure 7. Photographs of (a) hexadecane, (b) rapeseed oil, (c) glycerol, and (d) water droplets adhere to the PMF deposited substrates.